Journal of Animal Ecology

British Ecological Society

*Journal of Animal Ecology* 2014 doi: 10.1111/1365-2656.12257

# Overcompensation and phase effects in a cyclic common vole population: between first and second-order cycles

**Frédéric Barraquand[1,2]*†, Adrien Pinot[1,3]†, Nigel G. Yoccoz[2] and Vincent Bretagnolle[1]**

[1]*Centre d'Etudes Biologiques de Chizé, CNRS, Beauvoir-sur-Niort, France;* [2]*Department of Arctic and Marine Biology, University of Tromsø, Tromsø, Norway; and* [3]*VetAgro Sup, Campus agronomique de Clermont, Clermont-Ferrand, France*

## Summary

**1.** Population cycles in voles are often thought to be generated by one-year delayed density dependence on the annual population growth rate. In common voles, however, it has been suggested by Turchin (2003) that some populations exhibit first-order cycles, resulting from strong overcompensation (i.e. carrying capacity overshoots in peak years, with only an effect of the current year abundance on annual growth rates).

**2.** We focus on a common vole (*Microtus arvalis*) population from western France that exhibits 3-year cycles. Several overcompensating nonlinear models for populations dynamics are fitted to the data, notably those of Hassell, and Maynard-Smith and Slatkin.

**3.** Overcompensating direct density dependence (DD) provides a satisfactory description of winter crashes, and one-year delayed density dependence is not responsible for the crashes, thus these are not classical second-order cycles. A phase-driven modulation of direct density dependence maintains a low-phase, explaining why the cycles last three years instead of two. Our analyses suggest that some of this phase dependence can be expressed as one-year delayed DD, but phase dependence provides a better description. Hence, modelling suggests that cycles in this population are first-order cycles with a low phase after peaks, rather than fully second-order cycles.

**4.** However, based on the popular log-linear second-order autoregressive model, we would conclude only that negative delayed density dependence exists. The additive structure of this model cannot show *when* delayed DD occurs (here, during lows rather than peaks). Our analyses thus call into question the automated use of second-order log-linear models, and suggests that more attention should be given to non-(log)linear models when studying cyclic populations.

**5.** From a biological viewpoint, the fast crashes through overcompensation that we found suggest they might be caused by parasites or food rather than predators, though predators might have a role in maintaining the low phase and spatial synchrony.

**Key-words:** carrying capacity overshoots, density dependence, nonlinear, oscillatory dynamics, rodents

## Introduction

A common tenet in the study of population cycles, especially in small mammals, is that direct density dependence on the growth rate (i.e. immediate negative feedback) is stabilizing while delayed density dependence is destabilising (e.g. Ginzburg & Inchausti 1997; Stenseth 1999; Smith *et al.* 2006). For continuous-time models, this has been demonstrated many times thanks to the delayed logistic model and its spinoffs (e.g. Nisbet & Gurney 1982), thus the statement is correct when representing nature in continuous time through differential equations. However, most statistical models for voles and lemmings fluctuations are formulated in discrete time because of sampling constraints (annual or biannual sampling). In

*Correspondence author. E-mail: frederic.barraquand@uit.no
†Equal contribution

this context, the presence of one-year delayed density dependence means the current annual growth rate is affected by both the current density and the density one year before, which is generally written $r_t = \ln(N_{t+1} / N_t) = f(N_t, N_{t\text{-}1})$. To make sense of these dependencies, several authors such as Royama (1992) and Turchin (2003) popularized the notion of *process order*. First-order cycles occur when $r_t$ depends only on $N_t$, and second-order cycles occur when a dependence on $N_{t\text{-}1}$ is also needed to generate the observed cycles.

Discrete-time models of the form $N_{t+1} = R\ N_t\ f(N_t)$, where $f$ is a nonlinear function, are known to exhibit a wide range of dynamical behaviours from stable points to limit cycles to chaos (May 1974). This happens when they are overcompensating, i.e. $N_t\ f(N_t)$ decreases for large $N_t$ values, as in the Ricker or logistic map (but not the Beverton-Holt). Overcompensating density dependence (DD) allows for carrying capacity overshoots: the population can grow well above some critical density and is taken back much below one time step after, leading to large oscillations. Models that are linear on a log-scale (i.e. discrete Gompertz model, Royama 1992; Ives *et al.* 2003) can exhibit overcompensation (here, dampening oscillations amplified by noise), but are somewhat less appropriate than nonlinear models to model overcompensation, because they produce in this case unrealistically high population growth rates when population density is very low ($f(N_t) \sim 1/N_t^a$ with $a > 0$, which tends to infinity when $N_t$ tends to zero).

For the high maximum growth rates of many rodent populations ($r > 2$, and often $r > 4$, Turchin & Ostfeld 1997), discrete-time first-order models are often chaotic. It is important to note, however, that in the chaotic regime many of these models show large oscillations (May 1974), and these are amplified by stochasticity that interacts with deterministic skeletons to produce population cycles (Higgins *et al.* 1997; Ellner & Turchin 2005; Ranta, Kaitala & Lundberg 2006). And in general, we know that highly nonlinear direct DD can be mistaken for delayed DD, if models that are not flexible enough are fitted (Berryman & Lima 2007). To sum up, there is a large potential for first-order models to produce what we identify as population cycles in noisy vole data.

That being said, the addition of delayed DD widens much more the potential for cyclicity, and it is thought that second-order cycles (Ginzburg & Inchausti 1997; Stenseth 1999; Turchin 2003; Smith *et al.* 2006) provide an excellent description of the dynamics at work in several natural populations of rodents. The occurrence of delayed DD has been indeed very well documented in Fennoscandia for field voles (*Microtus agrestis*) and grey-sided voles (*Myodes rufocanus,* in Hokkaido as well, Stenseth *et al.* 2003), where the dominant hypothesis is that predation by weasels generates the cycle (Hanski, Hansson & Henttonen 1991; Stenseth, Bjørnstad & Falck 1996; Hanski *et al.* 2001). In these cases, the pattern observed is rather logical: crashes often occur on the second peak year, when the putative mustelid population has had time to build up (Stenseth, Bjørnstad & Falck 1996). The presence of such double-peaks (i.e. two consecutive years at peak level, see e.g. Hansen, Stenseth & Henttonen 1999) in some series provides very clear evidence for important delayed DD. If the crash was caused instead by direct DD, the population would have crashed after the first peak year; hence, double-peaks imply delayed DD. In this case, delayed DD creates the crashes (or more correctly, the causal agent generating delayed density dependence creates the crashes).

Because the case of northern Fennoscandian voles has been hugely influential in the rodent cycle literature (Stenseth 1999; Turchin 2003), it is generally believed that crashes created by delayed DD should be a common attribute of all cycling populations – or almost all (Turchin 2003). However, it is also possible that delayed DD maintains troughs rather than create crashes (Boonstra, Krebs & Stenseth 1998). The precise effect of delayed DD is very likely to have been overlooked, given that classic log-linear models (Royama 1992) have an additive structure that makes it difficult to distinguish between creating crashes or maintaining lows. The magnitude of the effect of delayed log-density is indeed the same at all levels of current log-density in log-linear models.

In many rodent populations, a strong first-order signal has been found, sometimes with overcompensation (crashes induced by direct DD), with a weaker second-order signal (see examples in Lima, Berryman & Stenseth 2006). In such cases, it seems therefore likely that delayed DD has a different role than creating crashes. Common voles (*Microtus arvalis*) are an excellent case study to look at direct vs. delayed DD: they have been argued to exhibit simple first-order dynamics by Turchin (2003), but Lambin, Bretagnolle & Yoccoz (2006) using the same time series and log-linear autoregressive models found evidence for delayed DD. Hence, it is of interest to check exactly what kind of density dependence is at play in common voles.

Here, we describe the case of a common vole population that exhibit three-year cycles with apparently marked overcompensation (Fig. 1, DS times series in Lambin, Bretagnolle & Yoccoz 2006). A possibility for such three-year cycles through overcompensation is that it takes two years at maximum growth speed for the population to grow above its carrying capacity, as mentioned by Turchin (2003), when discussing first-order cycles in *M. arvalis*. In larger herbivores, the famous Soay sheep has been shown to exhibit such cycles, that Grenfell *et al.* (1992) modelled using the Maynard-Smith and Slatkin (MSS) difference equation, whose S-shaped density dependence is more prompt to generate three-year cycles than other overcompensatory models (e.g. Ricker, Hassell forms). As we show in the following, the pattern is slightly different in *M. arvalis*, where aside from overcompensation we observe a low-phase (i.e. refractory period after the crash, Boonstra, Krebs & Stenseth 1998).

 

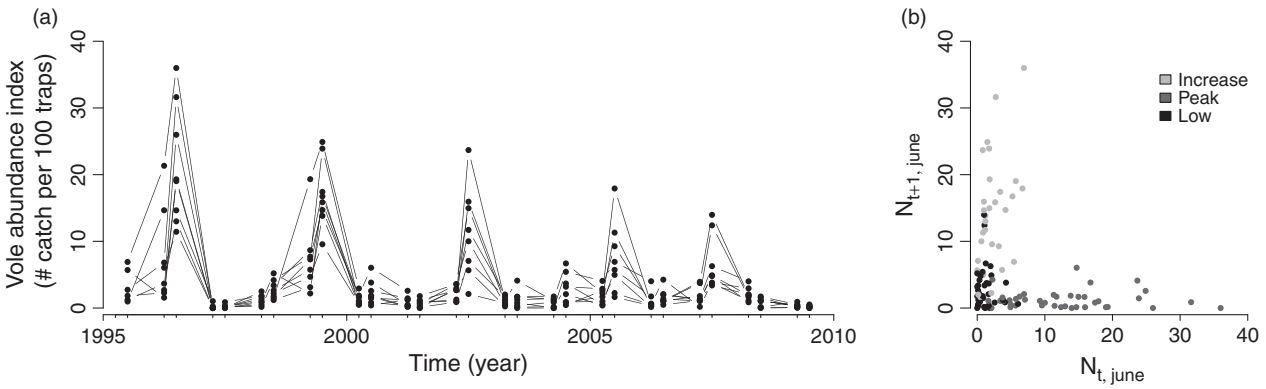


**Fig. 1.** (a) Times series of vole index, for the eight sectors of the study area. Each year, the first point represents April sampling and the second June sampling. June density index is taken as the baseline density to study annual population growth rates in this study. In (b), plot of next abundance ($N_{t+1}$) as a function of current abundance ($N_t$). Peak ($N_t > 5$), Low (year following peak), and Increase (other) years are plotted with different colours (Peak: dark grey; Low: black; Increase: light grey).

To study density dependence, one needs either long time series (e.g. Hansen, Stenseth & Henttonen 1999), or spatial replicates (Ims, Yoccoz & Killengreen 2011). Here, our time series is rather short, and we take advantage of spatial replication ($I = 8$ sectors, $T = 15$ years) to analyse population growth rates. Because we found evidence for nonlinear density dependence (including on a log-scale) we fit nonlinear discrete-time models through least squares, some of which include a dependence on the phase of the cycle to model the low-phase.

## Materials and methods

### STUDY SYSTEM

The common vole is an Eurasian rodent well-known for its outbreaks (Elton 1942; Jacob & Tkadlec 2010). The species has cyclic dynamics in many parts of Europe (Mackin-Rogalska & Nabagło 1990; Tkadlec & Stenseth 2001; Turchin 2003; Lambin, Bretagnolle & Yoccoz 2006; Jacob & Tkadlec 2010).

In agricultural areas, the common vole is generally an openfield rodent and lives in perennial crops (Briner, Nentwig & Airoldi 2005; Janova *et al.* 2011) but colonize cereals crops when sowed, where populations grow rapidly (Janova *et al.* 2011; Bonnet *et al.* 2013). However, agricultural practices such as mowing or ploughing are very detrimental to vole populations (Bonnet *et al.* 2013).

The study area, the LTER 'Zone Atelier Plaine & Val de Sèvre', covers 450 km$^2$ of intensive agricultural landscape located in western France (46°2′N, 0°4′W). Land use is dominated by winter cereals (42·0%), sunflower and maize (22·2%), rapeseed (8·9%), grassland (8·4%) and alfalfa (4·7%; all data from 2011). Trapping methods are described in Lambin, Bretagnolle & Yoccoz (2006); Inchausti *et al.* (2009); and Carslake *et al.* (2011). Briefly, sampling of common vole populations was carried out during two weeks long trapping sessions (in both April and June), from April 1995 to June 2009 (c. 5000 agricultural plots sampled). Nine sectors of similar size were defined in the study area for practical purposes (see Appendix S1, Supporting information), and 8 containing sufficient data are used here (the sampling continues >2009 but not with the same spatial resolution). For each sector and trapping session, 10 plots – comprising both grasslands and cereals) – were selected with a consistent design along a transect crossing the sector.

We performed our analyses on a reconstructed dataset comprising 1/4 grasslands (including Alfalfa) and 3/4 cereals. Given the abovementioned agricultural composition of the study area, this deserves some explanation. The sampling is biased towards crop types which contain voles during all the years, such as grasslands (23% of total trapping), alfalfa (22% of total), and cereals (21% of total. The rationale behind our (1/4, 3/4) simplification for grasslands (+alfalfa) and cereals is that if one excludes all other crop types (where voles are often poorly trapped or absent), in the remaining crop types, the share of annual crops (cereals) is 76%. We merge alfalfa and grasslands because they are rather similar crop types, although they do not have exactly the same phenology and cropping practices. The trapping index for vole abundance is the number of voles caught per 100 traps (only one night considered, Lambin, Bretagnolle & Yoccoz 2006; for an overview of the time series, see Fig. 1a).

### STATISTICAL ANALYSES

Due to the small length of the time series, we did not fit time-series models at the study area scale ($T = 17$ years at that scale). Instead, we took advantage of the spatial replication in the data set ($I = 8$ sectors, $T = 15$ years at that scale, see Appendix S1, Supporting information for a map with the sectors) to fit nonlinear models to annual population growth rates (PGRs) $r_t = \ln(N_{t+1}/N_t)$. This spatial scale is intermediate between that of the study area, where the time series is too short for most analyses using nonlinear models, and the spatial scale of the trapping line, where numerous zeros complicate the analysis (preliminary analyses using state-space models correcting for sampling variation on that dataset showed a bad fit, T. Cornulier pers. comm.; data set not included in Cornulier *et al.* 2013). Our choice of spatial scale therefore allowed to increase spatial replication while avoiding issues with zero values. We removed all the points for which the density was zero (only 12% of original dataset at the sector scale), rather than replace them by an arbitrary threshold which can strongly affect estimates of density dependence (Steen & Haydon 2000).

We fit direct and delayed density dependent functions on PGRs through a minimization of the residual sum of squares. It can be shown that this method is equivalent to maximum likelihood estimation of a population dynamics model assuming lognormal noise, using proper conditioning techniques on the likelihood (see e.g. Polansky *et al.* 2008, 2009). We checked that the nonlinear

 

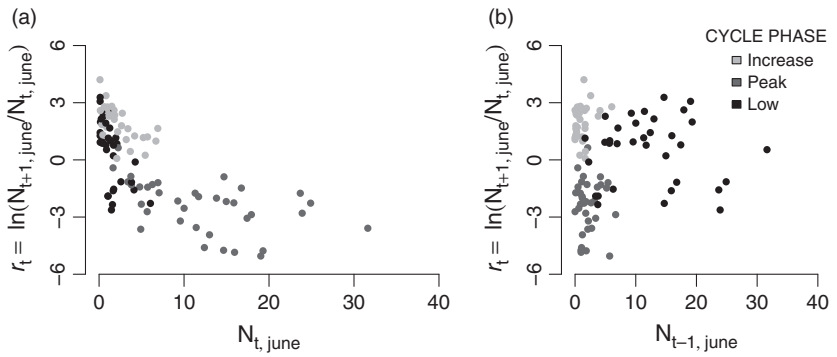


**Fig. 2.** June to June annual population growth rates (a) as a function of $N_t$ (June density) and (b) as a function of $N_{t\text{-}1}$ (past June density). Colours as in Fig. 1b.

optimisation algorithms were converging properly, which is important because of the occurrence of ridges in the likelihood with similar models (Polansky *et al.* 2008, 2009). We used the functions *nls( )* in R and *lsqcurvefit* in Matlab to fit the models. Surfaces of residuals sum of squares were also inspected, and some are reproduced in Appendix S2 (Supporting information). Confidence intervals presented in the main text are 999-bootstrapped confidence intervals at 95%. CIs have been produced using the R package *nlstools* designed to improve their robustness, and quantities bootstrapped are residuals from the regression, which in a spatiotemporal context improves performance (Lillegård, Engen & Sæther 2005). Our technique is akin to the surface response methodology (see Lindström *et al.* 1999; Turchin 2003; for details), except we fit models with parameters that can be biologically interpreted, rather than polynomial surfaces. We fit mostly models for direct density dependence of PGRs (see Statistical Models below and Fig. 2), later with different density dependence curves per phase. However, models including delayed density dependence are fitted as well in the last two sections of the results.

All models fitted assume that process error dominates observation error. As can be seen from Fig. 1 and has been later confirmed (Appendix S3, Supporting information), the residual spatial variance in population growth rates, that provides an upper bound for the observation error (used in e.g., Ives *et al.* 2008), is between a third and a half of the temporal variance.

Note that we do not fit explicitly spatial models, thus we do not estimate the associated spatial variance in PGRs in most cases (except in Appendix S3, Supporting information, using a version of the Hassell model with random effects). Thus, we cannot explicitly compute likelihood and consequently AIC. Additional simulations assuming process error dominates but that the observed spatial variation is present, followed by statistical model fitting, show that the simple nonspatial models provide nearly unbiased point estimates of parameters, though their precision is slightly affected by spatial replication (Appendix S3, Supporting information).

Model selection was performed in a two-step fashion: we first selected the models that gave the best fit in terms of sum of squares and not too wide confidence intervals for parameters, and then used leave one-out cross-validation (as recommended in e.g. Turchin 2003) to select the best models based with a predictive criterion, and therefore penalize over-parameterised models. This cross-validation is described below.

We use June vole abundance for all analyses on annual population growth rates and overcompensation. Although most analyses on voles are performed with autumn densities, sampling concentrated on June and April because cereals are harvested in summer and the ground is ploughed in autumn. Moreover, at this latitude June sampling gives summer abundance, because breeding mostly occurs before the relatively dry summer season. June abundance is therefore also used to determine the phase of the cycle in phase-dependent analyses. When June abundance ($N_t$) is above 5 voles per 100 trap-nights, we categorize the year as 'Peak', the following year is a 'Low', and the next year, preceding a peak, is categorized as 'Increase'. We followed this rule each year except for 2006–2007 when a 'Low' is directly followed by a 'Peak'. For phase-dependent models, PGR data was split into several sets according to the phase of the cycle.

## STATISTICAL MODELS

One has to pay attention to the exact shape of density dependence to understand the role of delayed DD: it is possible that a flexible polynomial model (e.g. Turchin 2003) includes a delayed density-dependent coefficient without delayed-density dependence being needed to explain the crashes. Therefore, we preferred to fit only models for which we had a biological interpretation of functional forms, based on the Hassell (1975) and Maynard Smith & Slatkin (1973) difference equations (multiplied by lognormal noise in eqns 1 and 2):

$$N_{t+1} = N_t \exp(r + \varepsilon_t)/(1 + N_t/K)^{\beta} \quad \text{eqn 1}$$

and

$$N_{t+1} = N_t \exp(r + \varepsilon_t)/(1 + (N_t/K)^{\gamma}) \quad \text{eqn 2}$$

where $r$ is the maximum PGR, $K$ a scale factor, $\beta$ and $\gamma$ shape parameters (for the Hassell and MSS models, respectively), and $\varepsilon_t \sim N(0,\sigma^2)$ a Gaussian random variable. The Maynard-Smith and Slatkin model (MSS) differs from the Hassell by the possibly sigmoid shape of density dependence, which allows more easily the creation of first-order cycles (as in the Soay sheep example, Grenfell *et al.* 1992). We also used variants including phase-dependent effects (below, models fitted in Figs 3 and 4) or delayed density dependence (see below and Appendix S4, Supporting information).

### *Phase-dependent models*

Because we were not fully satisfied with neither direct nor delayed density-dependent models (described in the next section), we used phase-dependent models (Stenseth 1999) to reproduce the low phase. Note that fitting density-dependent curves on three phases of a three-year cycle could here consistently produce three-year

 

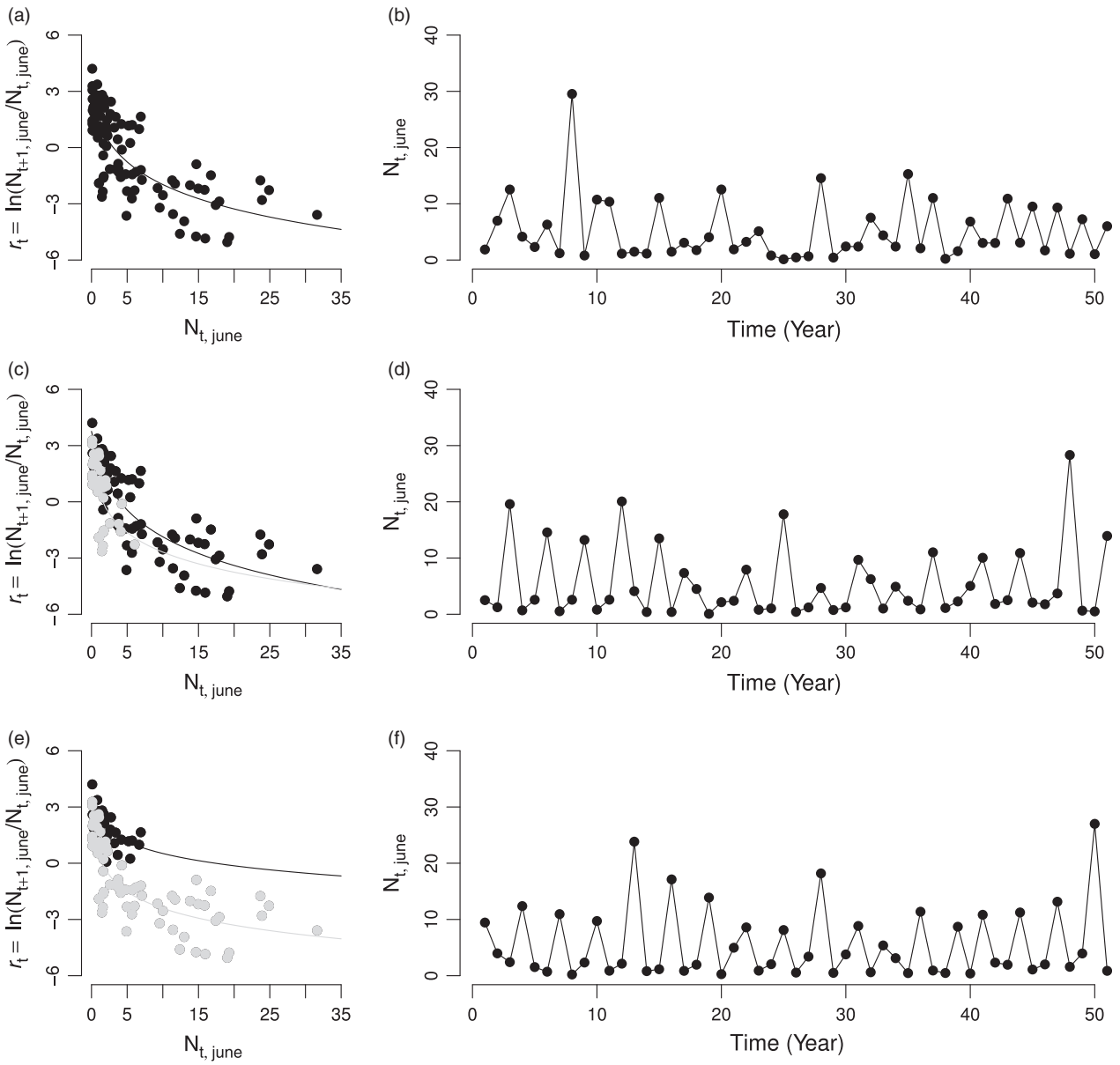


**Fig. 3.** (a) Nonlinear fit of Hassell model on the whole data set (b). Simulation of the resulting model (including stochasticity). Note that it is possible to obtain short sequences of three year cycles randomly given the level of stochasticity. (c) Nonlinear fit of Hassell model on Increase+Peak data (black points) and Low (grey points) (d) Simulation of the resulting model (including stochasticity). (e) Nonlinear fits of Hassell model on Increase data (black) and Peak+Low (grey) (f) Simulation of the resulting model (including stochasticity) – note this one looks consistently (i.e. across replicates) much closer to the observed time series.

cycles, irrespective of the type of density dependence estimated. This is because a simple ordered sequence of three mean growth rates is enough to generate a three-year cycle. Thus we separate the PGR data in only two groups.

In a first set of analyses, we fitted two density-dependent curves separately on the Low and Increase+Peak point clouds (L vs. IP). In a second step, we grouped Peak and Low together, and fit a density-dependent curve on the Increase phase separately (I vs. PL). We fitted both Hassell and MSS models. In the case of the MSS model, we realized that the Low data set was more logically modelled with a straight line (i.e., Ricker model, $r_t = r - \lambda N_t + \varepsilon_t$), which we then used for parsimony.

### *Delayed-density dependence*

To include the delayed density dependence that specifically generates the low phase, we derived a modified MSS model (eqn 3) where population growth is inhibited one year after the peak (large $N_{t-1}$ combined with low $N_t$ generates a low numerator).

$$N_{t+1} = N_t \exp(r - (aN_{t-1}/(1 + bN_t)) + \varepsilon_t)/(1 + (N_t/K)^{\gamma}) \qquad \text{eqn 3}$$

Another possibility to include a low phase is to translate the phase-dependent models into a delayed density-dependent

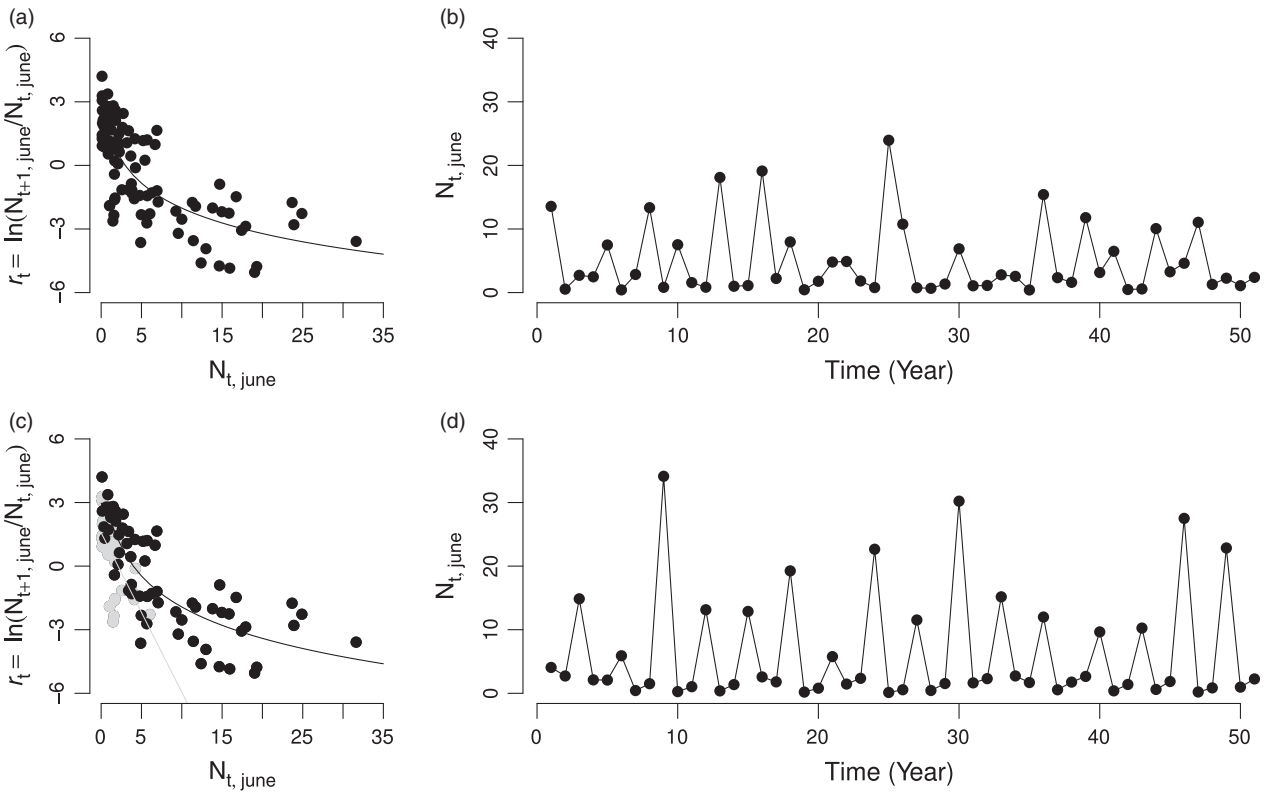


**Fig. 4.** (a) Nonlinear fit of Maynard-Smith and Slatkin (MSS) model on the whole data set. (b) Simulation of the resulting model (including stochasticity). Note that it is possible to obtain short sequences of three year cycles given the level of stochasticity. (c) Nonlinear fit of MSS and Ricker mixture model on Increase+Peak data (black points, MSS model fitted) and Low (grey points, Ricker model fitted) (d) Simulation of the resulting model (including stochasticity).

framework. In this case, we model explicitly how delayed density $N_{t-1}$ (rather than phase) changes the shape of direct density dependence (as done by Framstad *et al.* 1997; Stenseth *et al.* 1998; Stenseth 1999). Mathematically, this means introducing a function $\psi(N_{t-1})$ weighting both kinds of density-dependent functions:

$$N_{t+1} = N_t(\psi(N_{t-1})f(N_t) + (1 - \psi(N_{t-1}))g(N_t)) \qquad \text{eqn 4}$$

with $f(N_t) = \exp(r_1+\varepsilon_{t1}) / (1 + (N_t / K_1)^{\gamma})$ and $g(N_t) = \exp(r_2 (1 - N_t/K_2)+\varepsilon_{t2})$, as well as $\psi(N_{t-1}) = 1 / (1 + (N_{t-1}/5)^{\eta})$, where $\eta$ models the abruptness of the switch between both kinds of density dependence, and 5 [voles / 100 traps * nights] is the threshold density above which we define a peak.

For consistency with the published literature, we also compare the results of nonlinear models to those of log-linear models (as described in Royama 1992; Stenseth 1999), which fit less well, in Fig. 6 and Appendix S5 (Supporting information). The log-linear AR(1) and AR(2) models allow overcompensation to occur in some region of parameter space. The simplest AR(1) model writes

$$r_t = n_{t+1} - n_t = r_0 + \alpha n_t + \varepsilon_t \qquad \text{eqn 5}$$

with $n_t = \ln(N_t)$ and $\varepsilon_t \sim N(0,\sigma^2)$, or equivalently $N_{t+1} = N_t \exp(r_0 + \varepsilon_t) N_t^{\alpha}$.

## LEAVE-ONE-OUT CROSS-VALIDATION

To select models based on a balance between fit (measured by residual sum of squares) and predictive ability, which is key to compare the performance of first-order and phase-dependent models, we used a cross-validation technique. Due to data scarcity, we used the leave-one-out cross-validation recommended by Turchin (2003). The basic idea is to remove a data point from the initial dataset, fit the model on the rest of the dataset, and then try to predict the removed data point. To account for the fact that our dataset possesses spatial replication, we removed a whole year instead of one point in the plane (density, growth rate). This requires some explanation. We cannot just remove a data point (defined by both a sector and a year) because points belonging to different sectors for the same year are correlated. The principle of cross-validation is that the data being predicted must be independent of the data being fitted; removing only one data point would leave some information about that point in the rest of the data set; hence, we use a whole year.

Our technique can therefore be summarized as follows:

1. Remove data from year $t^*$ and create a data set $D^*_{ti} = (n_{ti} = \ln(N_{ti}), r_{ti}) \setminus (n_{t^*i}, r_{t^*i})$ with one less year
2. Fit all the models being compared on $D^*_{ti}$
3. Predict the next growth rate ($r^*_{ti}$) for all $i$ in [1:$I$] with the estimated models and compute the deviations to the observed growth rates, $r^*_{ti} - r_{ti}$.

4 Repeat for all years $t$ in [1:$T$] and compute $R^2_{pred} = 1 - \Sigma_{t,i} (r^*_{ti} - r_{ti})^2 / \Sigma_{t,i} (r_{ti} - r..)^2$, with $r..$ the overall mean.

The quantity $R^2_{pred}$, used in Turchin (2003), p. 195, is a measure of the predictive ability of the model. We include as supplement the full R -code for the analysis (see Data accessibility), which has been tested on simulated data.

## Results

### TEMPORAL PATTERNS AND EXPLORATION OF DENSITY DEPENDENCE

The pattern in Fig. 1 (a and b) clearly suggests overcompensation (i.e. densities after a peak are always much lower than at the peak). The population growth rates are presented in Fig. 2: direct density dependence is present (Fig. 2a), and varies according to cycle phase. Visually the evidence for one-year delayed density dependence seems weak in this dataset (Fig. 2b), even when accounting for cycle phase.

We initially expected a simple low-phase to explain the three year cycles, with inhibition of growth after a peak, i.e. $r_t$ values close to zero when $N_{t-1}$ is large. However, during the low phase, some PGRs are still positive, while others are not (Fig. 2a). The population dynamics models of the next section make clearer which elements are needed to reproduce the observed cycles.

### FIT OF NONLINEAR MODELS FOR DENSITY DEPENDENCE ON ANNUAL DATA

#### *Analyses with the Hassell model*

The Hassell model (eqn 1, curve in Fig. 3a) provided visually a good fit to the whole annual PGR dataset (points in Fig. 3a). Similar modelling hints based on the shape of the point cloud are presented in Saitoh, Stenseth & Bjørnstad (1997). Simulations of the model for estimated values are presented in Fig. 3b, and they already reproduce correctly the characteristic fast population crashes. Estimated parameters are [95% confidence intervals in brackets]: $r$ = 2·53 [1·80; 3·36], $\beta$ = 2·08 [1·45; 3·38], $K$ = 1·30 [0·40; 4·49], $\sigma$ = 1·43 (we used $\sigma$ = 1 in the simulation given that this error is overestimated, due to the presence of spatial variance in the data, see Appendix S3, Supporting information).

The first phase-dependent model (Hassell two-phase IP vs. L, Fig. 3c,d) corresponds to a low-phase that occurs because growth is inhibited by past peak densities. The second model I vs. PL (Fig. 3 e,f) corresponds in contrast to a low-phase occurring because growth only occurs when both current and delayed densities are low. The fit of the first model IP vs. L (Fig. 3c) shows relatively similar density-dependent curves; therefore, low improvement in fit due to the phase-dependent analysis of density dependence, with dynamics (Fig. 3d) similar to the uniphase Hassell model (Fig. 3b). Parameters of IP (black): $r$ = 3·77 [2·47; 3·94], $\beta$ = 2·39 [1·69; 4·01], $K$ = 1·05 [0·08; 4·90], $\sigma$ = 0·71 ($\sigma$ = 0·5 in simulation) and in Low phase (grey): $r$ = 2·59 [1·46; 5·72], $\beta$ = 1·83 [0·91; 12·87] CI60 [1·29; 3·19], $K$ = 0·48 [0·01; 12·35] CI60 [0·18; 1·80], $\sigma$ = 1·322 ($\sigma$ = 1 in simulation).

On the other hand, the second set of analyses (I vs. PL model) clearly delineates two types of density dependence (Fig. 3e) and simulation of the model yields a cycle rather close to the observed dynamics (Fig. 3f, with a low phase). Fig 3e shows that density dependence is still strong during the low phase (contrary to our initial expectations); local populations that have rebounced from low values after the peak can still be influenced by direct density dependence. Parameters of I phase (black): $r$ = 3·25 [2·49; 4·66], $\beta$ = 1·05 [0·52; 9·86] CI60 [0·74;1·81], $K$ = 0·75 [0·00; 26·96] CI60 [0·16;2·62], $\sigma$ = 1·32 ($\sigma$ = 1 in simulation) and PL phase (grey) $r$ = 2·77 [150;5·51], $\beta$ = 1·37 [1·07;1·94], $K$ = 0·22 [0·00; 1·19], $\sigma$ = 1·32 (1 in simulation). Note the errors are indeed both equal to 1·32.

#### *Analyses with the Maynard-Smith and Slatkin model*

As we did not find a sigmoid pattern of density dependence in the whole point cloud, we initially favoured the Hassell model to the MSS model (eqn 2). When fitting the MSS model to the whole data set, however, one realises the quality of fit is similar to that of the Hassell model (Table 1, Fig. 4a). Estimated parameters are: $r$ = 2·25 [1·53; 3·13], $\gamma$ = 1·75 [1·38; 2·23], $K$ = 0·89[0·31; 1·90], $\sigma$ = 1·42 ($\sigma$ = 1 in the simulation). The inflection point of this model (i.e. the threshold density value that connects both concave and convex parts) is very low, which means the concave part is restricted to very low densities and the shape of density dependence is rather similar to that of eqn 1. Simulations of the model yield a cycle close to the observed dynamics (Fig. 4b).

We found that a sigmoid model may fit better the IP point cloud while a straight line would fit correctly the L cloud (i.e. Ricker model $r_t = r - \lambda N_t + \varepsilon_t$), as shown in Fig 4c. Parameters of IP (black in Fig 4c) are: $r$ = 3·03 [2·04; 4·47], $\gamma$ = 2·16 [1·73; 2·68], $K$ = 1·01 [0·32; 2·09], $\sigma$ = 1·31 ($\sigma$ = 1 in simulation) and L (grey): $r$ = 1·57 [0·87;2·28], $\lambda$ = 0·74 [0·43; 1·11], $\sigma$ = 1·40 ($\sigma$ = 1 in simulation). According to its residual sum of squares (Table 1), the model performs better than Hassell IP vs. L, though it performs worse than Hassell I vs. PL. However, the precision of estimates (width of 95% confidence intervals) is much higher here (legend of Fig. 4). Therefore, this two-phase model MSS: IP / Ricker: L appears to be a suitable representation of the population dynamics, with here again, a low phase marked by strong direct density dependence.

### DELAYED DENSITY DEPENDENT AND RESPONSE SURFACE FORMULATION

The quality of fit as measured by RSS of the model in eqn 3 is similar to phase-dependent models, though

**Table 1.** Residual sum of squares (RSS) for the various models considered. The sum of squared deviations to the mean is 521, which implies the models explained around 60% of the variability in the data ($R^2$) for the uniphase Hassell and Maynard-Smith and Slatkin (MSS) models, and up to nearly 80% for the more complex two-phase models. RSS and number of parameters for the uniphase models are presented in italics. When two phases are considered we evaluate model fit by summing the two RSS (in the first column, total number of parameters in bold in the second column). The best fitting model is the two-phase Hassell (Peak+Low, Increase), but it contains one additional parameter when compared to the combination MSS (Increase+Peak) and Ricker (Low)

| | Hassell | | MSS | |
|---|---|---|---|---|
| Model | RSS | Parameters | RSS | Parameters |
| Total (no phase) | 202·4 | **3** | 202·3 | **3** |
| Increase | *13·8* | *3* | | |
| Peak+Low | *99·5* | *3* | | |
| Total (Peak+Low, Increase) | 113·3 | **6** | | |
| Increase+Peak | *111·8* | *3* | *109·5* | *3* |
| Low (Ricker) | *55·9* | *3* | *62·7 (linear fit)* | *2* |
| Total (Increase+Peak, Low) | 167·7 | **6** | 172·2 | **5** |

slightly poorer. However, simulations do not reproduce very well the observed dynamics (see Appendix S4, Supporting information).

The delayed density equivalent of the phase dependent models, mathematically described by eqn 4, does not improve the fit nor model realism, because $\eta$ is always estimated around 1. As $\eta$ should be around 5 to produce a clear switch between both kinds of DD, this model reproduces poorly the data during simulations, and the phase-dependent representation is therefore a simpler and more efficient way of representing the data than eqn 4.

### SEASONAL PATTERNS OF DENSITY DEPENDENCE

The annual pattern of density dependence is largely driven by June-to-April PGRs (encompassing the important winter season). We know that crashes occur during the real winter season (November to February) from observations and additional winter trapping (Pinot *et al*. unpublished). Spring growth rates (April to June) are on average positive and driven by environmental stochasticity, though direct density dependence is also present, sometimes generating crashes (Fig 5a).

No one-year delayed density dependence has been found in either spring or winter growth rates (Fig 5b), and the phase-dependent pattern of direct density dependence maintains itself in winter growth rates (Fig 5c). This concurs with the pattern found in annual data: first-order cycles with some phase-dependent modulation of direct density dependence.

### PITFALLS OF LOG-LINEAR MODELLING

The parameters of the AR(1) model (eqn 5) are estimated to $r_0 = 0{\cdot}92$ [0·56; 1·27], $\alpha = -1{\cdot}18$ [−1·39; −0·98], $\sigma = 1{\cdot}48$. Overcompensation occurs whenever $\alpha < -1$ (Ives *et al*. 2003), and more stable dynamics when $-1 < \alpha < 0$. Here, we observe therefore overcompensation according to the AR(1) model too. The AR(2) model, in turn, display cycles of 2–4 years in the parameter region where it overcompensates (Royama 1992; left side of the parameter triangle), depending on the value of the delayed DD coefficient. Therefore, AR(2) models could in theory describe the dynamics occurring here (see Appendix S5, Supporting information). However, when these models exhibit overcompensation (first coefficient $<-1$), the maximum population growth rate (when $N_t$ tends to zero) is infinite (Fig. 6c), which produces very fast increases when used to simulate data (faster than we observe in the data set, see Appendix S5, Supporting information). Another unrealistic feature is that some declines occur in two years rather than one (Appendix S5, Supporting information). This is because in the log-linear AR(2) model, the delayed density dependence is purely additive, i.e. has the same effect on the population growth rate when current log-density is high or low (Appendix S5, Supporting information). Because we aim at modelling cycles using empirically-motivated functional forms and respecting biological constraints, we prefer the nonlinear models.

### OVERVIEW AND LEAVE-ONE-OUT CROSS-VALIDATION

Comparing sum of squares shows that in terms of fit, MSS and Hassell models are similar (Table 1). We also see that there is a clear improvement when considering two-phase models: the $R^2$ increases from c. 60% to 80% (with, of course, an increase in the number of parameters, Table 1).

We eliminated the Hassell two-phase model from the final model set for cross validation because of its too wide confidence intervals, and other delayed density-dependent models that fitted less well or had inappropriate structure. We therefore considered that three models of varying complexity provided reasonable descriptions of our dataset: the MSS, Hassell and MSS (IP)/Ricker (L) mixture. Their $R^2_{\text{pred}}$ are, respectively, 0·515, 0·513 and 0·53. Hence, the cross-validation procedure still favours the MSS/Ricker mixture including a low phase, but only slightly.

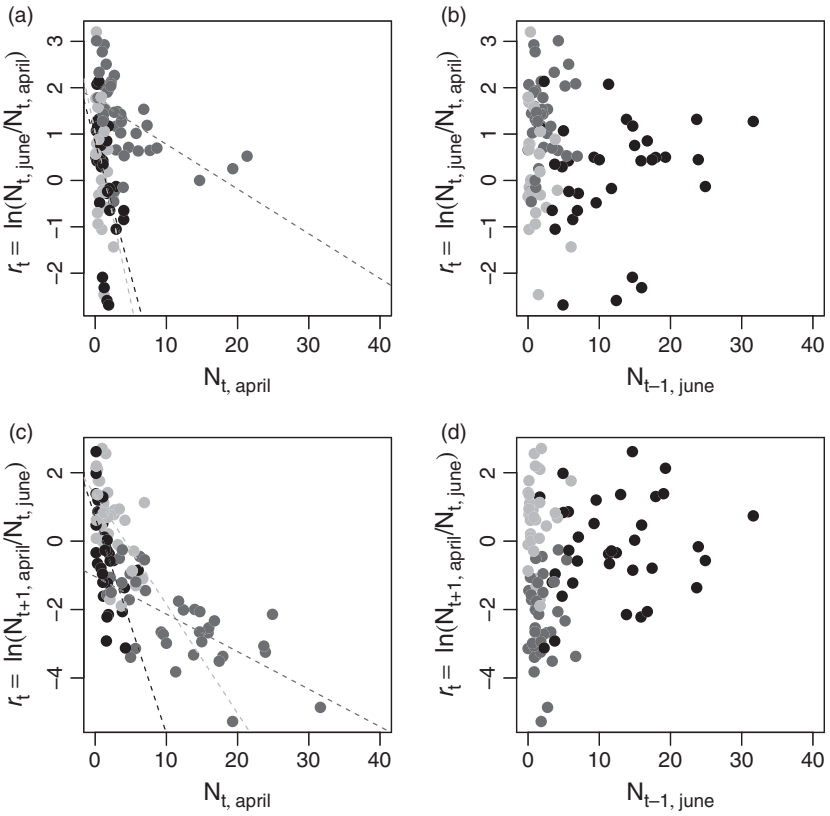


**Fig. 5.** Seasonal growth rates. Direct density dependence in the spring (a), c. 25% of explained variability. Colours are as in Fig 1b, and the Peak category refers here to the summer density that follows the considered spring. Delayed density dependence on spring growth rates is absent (b). 'Winter' growth rates (June to next April) show the same density-dependent pattern as in the annual data (c); and no discernable delayed density dependence (d).

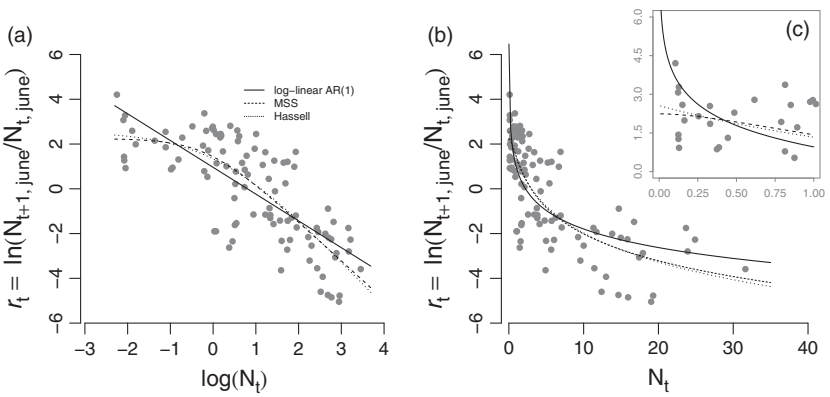


**Fig. 6.** Fit of a log-linear AR(1) model (filled line), and comparison to the models of Hassell (dashed) and Maynard-Smith and Slatkin (dotted). In (a), the fit is represented in a logarithmic scale, and in (b) in the regular abundance scale. We plotted in (c) a zoom of small $N_t$ values, showing nonlinear models allow for more realistic finite values of the maximum growth rate at low densities.

## Discussion

Statistical modelling has been used extensively in the population cycles literature to infer potential biological mechanisms (Bjørnstad, Falck & Stenseth 1995; Turchin 2003). Many biological explanations of population cycles are however possible due to the scarcity of community-level data. Hence, it is paramount to ensure the robustness of the models developed. For that reason, we focus on methodological issues first and after on the biological interpretation of the results.

The density-dependent models we fitted are quite robust in terms of both parameter estimates, as $r$ is always estimated in the range 2–3 and $\beta$ or $\gamma$ in the range 1·5–2·5, as well as dynamical behaviour (cycles of correct observed periodicity and asymmetric shape). The overall pattern that emerges from our analyses is that crashes are generated by overcompensating direct density dependence (as shown by density-dependent exponents $\beta$ and $\gamma > 1$). Populations could in theory, if they grew at the maximum observed rate, reach again peak levels in one year (and they did in 2007, see Fig. 1a) but often a low phase remains after the peak, which therefore involves delayed or phase-driven density dependence (DD).

### ON THE ORDER OF DENSITY DEPENDENCE IN COMMON VOLES

The observed patterns of DD are in contrast to many northern field vole (*Microtus agrestis*) and grey-sided vole (*Myodes rufocanus*) populations, where a stronger delayed DD signature and longer cycles are observed (e.g. Hansen,

Stenseth & Henttonen 1999), with delayed DD leading to crashes rather than just maintaining lows like here. This is evident from the fact that many Northern vole populations can sometime stay 2 years (or 3, more rarely) at the peak (e.g. Hansen, Stenseth & Henttonen 1999). These differences between common voles and their northern cousins led Turchin (2003) to suggest that common voles have mostly first-order cycles. However, Lambin, Bretagnolle & Yoccoz (2006) found delayed DD on the same time series we examine here (called DS in Lambin, Bretagnolle & Yoccoz 2006), using log-linear models, and suggested second-order cycles. One might then wonder what sort of cycles are present in Western France, given that differences in process order can point to different cycle-generating mechanisms.

Using more refined non-linear models and an extended dataset, we reconcile the findings of Turchin (2003) and Lambin, Bretagnolle & Yoccoz (2006), and show that the reality is somewhere in-between. Though there is a strong first-order signal of overcompensation that produces crashes, there is also an influence of one-year delayed density on annual PGRs that maintains lows. We were able to better detect the precise role of delayed DD with non-linear models, because classical log-linear AR(2) models simply cannot differentiate the various roles of delayed density dependence. Our findings therefore echo the warnings of Stenseth (1999) who suggested more attention should be given to nonlinearities. Although the classical log-linear AR(2) model remains a valuable tool, estimates of negative one-year delayed DD in this model should not be taken as proof that delayed DD is key to the cycles observed. Although we developed some models with delayed density dependence that fitted the data quite well, model simulations favoured phase-dependent models showing more realistic dynamics. That is, delayed density dependence is actually better described as a phase dependence of direct density dependence (see Results and Stenseth 1999). We believe this is partly related to the large-scale synchrony present here, which makes phase or past total abundance over a large area more relevant than past local abundance to determine the shape of direct density dependence.

For instance, after a peak year over the entire study area, a sector in which the vole peak is only moderate will be subjected to strong direct density dependence even though local abundance might not be so high. Previous research on patterns of synchrony across species on the study area indicated that spatial synchrony is likely to be maintained at least in part by wide-ranging predators (Carslake *et al.* 2011), making such spillover effects across sectors possible (sectors are contiguous and a dozen $km^2$). Therefore, here as well we concur with Stenseth (1999) who favours a phase-dependent description of population dynamics (though we did not use threshold autoregressive log-linear models, as he and his co-authors did). Interestingly, phase dependence of density dependence has also been recently shown by Goswami *et al.* (2011) in prairie voles, a rather ecologically similar vole species. We note however that the improvement in terms of predictive performance for the model with a low-phase is rather low; only more data collection will tell us if a low-phase persists in this region, and is a genuine feature of the cycles.

### EXTENSIONS TO OTHER CYCLIC SPECIES, AND CYCLE CAUSATION

There is evidence in some lemming populations (of the *Lemmus* genus) of strong overcompensation (e.g. in Finse, Norway, Framstad *et al.* 1997; Kausrud *et al.* 2008), with characteristic sharp peaks and a low phase, generating overall a skewed distribution of abundance values (Turchin *et al.* 2000). Thus, Norwegian and brown lemmings (*Lemmus lemmus* and *Lemmus trimucronatus*) are prime candidates for similar modelling analyses, and models fitted to populations for Norwegian lemmings show that one-year delayed density dependence is also maintaining lows rather than creating crashes (Barraquand and Yoccoz, unpublished). In voles, Lima, Berryman & Stenseth (2006) suggested that the first-order feedback is stronger than the second-order feedback in many populations, thus similar analyses to ours could be done on other vole populations, including in Fennoscandia.

It is worthwhile noticing that delayed density dependence is sometimes branded a key component of population cycles on an annual basis (Stenseth 1999) and sometimes on a semi-annual basis (Hörnfeldt 1994). In Hörnfeldt (1994), delayed DD refers to the dependence of the 6-month PGR on the densities one season before. Such seasonal delayed DD translate at the annual scale into annual delayed DD only if both seasons are affected (relations between seasonal and annual PGRs, based on log-linear models, are shown in Hansen, Stenseth & Henttonen 1999). We encourage other authors to state clearly the timelag they consider (e.g. one month in Goswami *et al.* 2011), and to scale up when possible to the annual scale, which is the common denominator of all cyclic vertebrate datasets.

In contrast to Ergon *et al.* (2011), who studied field voles, we did not find one-year delayed density dependence on the spring growth rates. Both decreased winter survival and reproduction in peak years are likely culprits for the crashes (given that declines happen in winter here). Though predation is likely to be involved in the synchronization of local vole dynamics, what causes the winter crashes, and therefore the oscillatory dynamics, is currently unknown. The fact that direct DD, and not delayed DD, is creating the crashes points to other causal agents than specialist predators (mustelids; see Discussion in Lambin, Bretagnolle & Yoccoz 2006).

Many causal agents may be invoked to explain population crashes, such as parasites which benefit from high transmission rates at the promiscuity induced by high densities (Anderson & May 1980). This mechanism was

 

advanced long ago on the basis of microbiological analyses to explain common vole crashes in North-Western France (Regnier & Pussard 1926). Food shortages in winter – proposed for that species by Turchin (2003), or aggregating generalist predators (Ims & Steen 1990) are also plausible hypotheses. However, estimates of outbreak vole population densities in winter often exceed 800 voles per ha at the scale of agricultural fields, suggesting that generalist predation is unlikely to initiate the crashes.

This leaves food, parasites, or any interaction of these two factors (as highlighted in Pedersen & Greives 2008), but more demographic and physiological data need to be collected before any tentative answer is proposed for the puzzling crashes of common voles.

## Acknowledgements

We thank numerous fieldworkers who contributed to this study, especially Bertrand Gauffre who organised sampling since 2006, and Thomas Cornulier and Xavier Lambin for discussions. FB's postdoc was funded by the program Biodiversa ECOCYCLES and AP was funded by a PhD grant from University of Paris 6. Thanks to Florian Hartig and two reviewers for constructive comments that considerably strengthened the manuscript.

## Data accessibility

The data and the computer codes are available from the Dryad repository, doi:10.5061/dryad.2hk46 (Barraquand *et al.* 2014).

## References

Anderson, R.M. & May, R.M. (1980) Infectious diseases and population cycles of forest insects. *Science*, **210**, 658–661.

Barraquand, F., Pinot, A., Yoccoz, N.G. & Bretagnolle, V. (2014) Overcompensation and phase effects in a cyclic common vole population: between first and second-order cycles. Dryad Digital Repository, doi:10.5061/dryad.2hk46.

Berryman, A. & Lima, M. (2007) Detecting the order of population dynamics from time series: nonlinearity causes spurious diagnosis. *Ecology*, **88**, 2121–2123.

Bjørnstad, O.N., Falck, W. & Stenseth, N.C. (1995) A geographic gradient in small rodent density fluctuations: a statistical modelling approach. *Proceedings of the Royal Society of London Series B: Biological Sciences*, **262**, 127–133.

Bonnet, T., Crespin, L., Pinot, A., Bruneteau, L., Bretagnolle, V. & Gauffre, B. (2013) How the common vole copes with modern farming: insights from a capture–mark–recapture experiment. *Agriculture, Ecosystems & Environment*, **177**, 21–27.

Boonstra, R., Krebs, C.J. & Stenseth, N.C. (1998) Population cycles in small mammals: the problem of explaining the low phase. *Ecology*, **79**, 1479–1488.

Briner, T., Nentwig, W. & Airoldi, J.P. (2005) Habitat quality of wildflower strips for common voles (Microtus arvalis) and its relevance for agriculture. *Agriculture, Ecosystems & Environment*, **105**, 173–179.

Carslake, D., Cornulier, T., Inchausti, P. & Bretagnolle, V. (2011) Spatio-temporal covariation in abundance between the cyclic common vole *Microtus arvalis* and other small mammal prey species. *Ecography*, **34**, 327–335.

Cornulier, T., Yoccoz, N.G., Bretagnolle, V., Brommer, J.E., Butet, A., Ecke, F. *et al.* (2013) Europe-wide dampening of population cycles in keystone herbivores. *Science*, **340**, 63–66.

Ellner, S.P. & Turchin, P. (2005) When can noise induce chaos and why does it matter: a critique. *Oikos*, **111**, 620–631.

Elton, C. (1942). Voles, mice and lemmings. Problems in population dynamics. Clarendon Press, Oxford, United Kingdom.

Ergon, T., Ergon, R., Begon, M., Telfer, S. & Lambin, X. (2011) Delayed density-dependent onset of spring reproduction in a fluctuating population of field voles. *Oikos*, **120**, 934–940.

Framstad, E., Stenseth, N.C., Bjørnstad, O.N. & Falck, W. (1997) Limit cycles in Norwegian lemmings: tensions between phase–dependence and density-dependence. *Proceedings of the Royal Society of London Series B: Biological Sciences*, **264**, 31–38.

Ginzburg, L.R. & Inchausti, P. (1997) Asymmetry of population cycles: abundance-growth representation of hidden causes of ecological dynamics. *Oikos*, **80**, 435–447.

Goswami, V.R., Getz, L.L., Hostetler, J.A., Ozgul, A. & Oli, M.K. (2011) Synergistic influences of phase, density, and climatic variation on the dynamics of fluctuating populations. *Ecology*, **92**, 1680–1690.

Grenfell, B.T., Price, O.F., Albon, S.D. & Clutton-Brock, T.H. (1992) Overcompensation and population cycles in an ungulate. *Nature*, **355**, 823–826.

Hansen, T.F., Stenseth, N.C. & Henttonen, H. (1999) Multiannual vole cycles and population regulation during long winters: an analysis of seasonal density dependence. *The American Naturalist*, **154**, 129–139.

Hanski, I., Hansson, L. & Henttonen, H. (1991) Specialist predators, generalist predators, and the microtine rodent cycle. *Journal of Animal Ecology*, **60**, 353–367.

Hanski, I., Henttonen, H., Korpimäki, E., Oksanen, L. & Turchin, P. (2001) Small-rodent dynamics and predation. *Ecology*, **82**, 1505–1520.

Hassell, M.P. (1975) Density-dependence in single-species populations. *Journal of Animal Ecology*, **44**, 283–295.

Higgins, K., Hastings, A., Sarvela, J.N. & Botsford, L.W. (1997) Stochastic dynamics and deterministic skeletons: population behavior of *Dungeness crab*. *Science*, **276**, 1431–1435.

Hörnfeldt, B. (1994) Delayed density dependence as a determinant of vole cycles. *Ecology*, **75**, 791–806.

Ims, R.A. & Steen, H. (1990) Geographical synchrony in microtine population cycles: a theoretical evaluation of the role of nomadic avian predators. *Oikos*, **57**, 381–387.

Ims, R.A., Yoccoz, N.G. & Killengreen, S.T. (2011) Determinants of lemming outbreaks. *Proceedings of the National Academy of Sciences*, **108**, 1970–1974.

Inchausti, P., Carslake, D., Attié, C. & Bretagnolle, V. (2009) Is there direct and delayed density dependent variation in population structure in a temperate European cyclic vole population? *Oikos*, **118**, 1201–1211.

Ives, A.R., Dennis, B., Cottingham, K.L. & Carpenter, S.R. (2003) Estimating community stability and ecological interactions from time-series data. *Ecological monographs*, **73**, 301–330.

Ives, A.R., Einarsson, Á., Jansen, V.A. & Gardarsson, A. (2008) High-amplitude fluctuations and alternative dynamical states of midges in Lake Myvatn. *Nature*, **452**, 84–87.

Jacob, J., Tkadlec, E. (2010). Rodent outbreaks in Europe: dynamics and damage. *Rodent Outbreaks: Ecology and Impacts* (eds G.R. Singleton, S.R. Belmain, P.R. Brown & B. Hardy.), pp. 207–223. International Rice Research Institute, Los Baños, Philippines.

Janova, E., Heroldova, M., Konecny, A. & Bryja, J. (2011) Traditional and diversified crops in South Moravia (Czech Republic): habitat preferences of common vole and mice species. *Mammalian Biology-Zeitschrift für Säugetierkunde*, **76**, 570–576.

Kausrud, K.L., Mysterud, A., Steen, H., Vik, J.O., Østbye, E., Cazelles, B. *et al.* (2008) Linking climate change to lemming cycles. *Nature*, **456**, 93–97.

Lambin, X., Bretagnolle, V. & Yoccoz, N.G. (2006) Vole population cycles in northern and southern Europe: is there a need for different explanations for single pattern? *Journal of Animal Ecology*, **75**, 340–349.

Lillegård, M., Engen, S. & Sæther, B.E. (2005) Bootstrap methods for estimating spatial synchrony of fluctuating populations. *Oikos*, **109**, 342–350.

Lima, M., Berryman, A. & Stenseth, N.C. (2006) Feedback structures of northern small rodent populations. *Oikos*, **112**, 555–564.

Lindström, J., Kokko, H., Ranta, E. & Lindén, H. (1999) Density dependence and the response surface methodology. *Oikos*, **85**, 40–52.

Mackin-Rogalska, R. & Nabagło, L. (1990) Geographical variation in cyclic periodicity and synchrony in the common vole, *Microtus arvalis*. *Oikos*, **59**, 343–348.

May, R.M. (1974) Biological populations with nonoverlapping generations: stable points, stable cycles, and chaos. *Science*, **186**, 645–647.

Maynard Smith, J. & Slatkin, M. (1973) The stability of predator-prey systems. *Ecology*, **54**, 384–391.

Nisbet, R.M. & Gurney, W.S.C. (1982) *Modelling Fluctuating Populations*. Wiley, New York, USA.

Pedersen, A.B. & Greives, T.J. (2008) The interaction of parasites and resources cause crashes in a wild mouse population. *Journal of Animal Ecology*, **77**, 370–377.
Polansky, L., de Valpine, P., Lloyd-Smith, J.O. & Getz, W.M. (2008) Parameter estimation in a generalized discrete-time model of density dependence. *Theoretical Ecology*, **1**, 221–229.
Polansky, L., De Valpine, P., Lloyd-Smith, J.O. & Getz, W.M. (2009) Likelihood ridges and multimodality in population growth rate models. *Ecology*, **90**, 2313–2320.
Ranta, E., Kaitala, V. & Lundberg, P. (2006) *Ecology of Populations*. Cambridge University Press, New Jersey, USA.
Regnier, R. & Pussard, R. (1926) Le Campagnol des champs (*Microtus arvalis Pall.*) et sa destruction. *Annales des Épiphyties*, **12**, 385–525.
Royama, T. (1992) *Analytical Population Dynamics*. Chapman and Hall, London, UK.
Saitoh, T., Stenseth, N.C. & Bjørnstad, O.N. (1997) Density-dependence in fluctuating grey-sided vole populations. *Journal of Animal Ecology*, **66**, 14–24.
Smith, M.J., White, A., Lambin, X., Sherratt, J.A. & Begon, M. (2006) Delayed density-dependent season length alone can lead to rodent population cycles. *The American Naturalist*, **167**, 695–704.
Steen, H. & Haydon, D. (2000) Can population growth rates vary with the spatial scale at which they are measured? *Journal of Animal Ecology*, **69**, 659–671.
Stenseth, N.C. (1999) Population cycles in voles and lemmings: density dependence and phase dependence in a stochastic world. *Oikos*, **87**, 427–461.
Stenseth, N.C., Bjørnstad, O.N. & Falck, W. (1996) Is spacing behaviour coupled with predation causing the microtine density cycle? A synthesis of current process-oriented and pattern-oriented studies *Proceedings of the Royal Society of London Series B: Biological Sciences*, **263**, 1423–1435.
Stenseth, N.C., Chan, K., Framstad, E. & Tong, H. (1998) Phase-and density-dependent population dynamics in Norwegian lemmings: interaction between deterministic and stochastic processes. *Proceedings of the Royal Society of London. Series B: Biological Sciences*, **265**, 1957–1968.
Stenseth, N.C., Viljugrein, H., Saitoh, T., Hansen, T.F., Kittilsen, M.O., Bølviken, E. *et al.* (2003) Seasonality, density dependence, and population cycles in Hokkaido voles. *Proceedings of the National Academy of Sciences*, **100**, 11478–11483.
Tkadlec, E. & Stenseth, N.C. (2001) A new geographical gradient in vole population dynamics. *Proceedings of the Royal Society of London Series B: Biological Sciences*, **268**, 1547–1552.
Turchin, P. (2003) *Complex Population Dynamics: A Theoretical/Empirical Synthesis*. Princeton University Press, Princeton, New Jersey, USA.
Turchin, P. & Ostfeld, R.S. (1997) Effects of density and season on the population rate of change in the meadow vole. *Oikos*, **78**, 355–361.
Turchin, P., Oksanen, L., Ekerholm, P., Oksanen, T. & Henttonen, H. (2000) Are lemmings prey or predators? *Nature*, **405**, 562–565.

*Received 27 August 2013; accepted 29 May 2014*
*Handling Editor: Tim Coulson*

## Supporting Information

Additional Supporting Information may be found in the online version of this article.

**Appendix S1.** Spatiotemporal dynamics of common voles

**Appendix S2.** Surfaces of residual sum of squares (RSS)

**Appendix S3.** Spatial and temporal variance in population growth rates

**Appendix S4.** Fit of response surface models in the plane ($N_t$, $N_{t-1}$)

**Appendix S5.** Fit of log-linear models on population growth rates